Effect—and removal—of an ultrashort pulse's spatial profile on the single-shot measurement of its temporal profile

Dongjoo Lee,* Ziyang Wang, Xun Gu, and Rick Trebino

Georgia Institute of Technology, School of Physics, Atlanta, Georgia 30332, USA
*Corresponding author: Dongjoo.lee@swampoptics.com

Because single-shot ultrashort-pulse-measurement methods usually map delay onto the transverse spatial coordinate, a nonuniform pulse spatial profile could badly distort the measurement versus delay. Furthermore, beam-induced distortions could occur in techniques, such as GRENOUILLE, in which the pulse frequency is mapped to the angular coordinate in the orthogonal direction. We study these effects in the frequency-resolved-optical-gating (FROG) and GRENOUILLE techniques and show that they are considerably reduced by fortuitous aspects of, in particular, the GRENOUILLE beam geometry in practice. Also, we show that it is possible to remove both of these distortion effects by simply dividing the trace by a simple function of the beam input spatial profile. We demonstrate these (small) effects and their removal in GRENOUILLE measurements. © 2008 Optical Society of America

OCIS codes: 320.0320, 320.7100.

1. SINGLE-SHOT VERSUS MULTISHOT PULSE MEASUREMENT

Variations in the spatial profile of an ultrashort pulse are generally neglected when measuring its temporal profile. This is not usually a problem in multishot measurements of ultrashort pulses, in which the delay is typically scanned by moving a mirror, and, as long as spatiotemporal distortions are absent (that is, the pulses' spatial and temporal field dependences separate), the spatial dependence of the field factors out of the expression for the pulse autocorrelation and frequency-resolved-optical-gating (FROG) [1] trace. As a result, multishot autocorrelation and FROG measurements are essentially immune to poor spatial mode quality. However, multishot methods require scanning the delay, which can be slow and laborious. Multishot methods also suffer from geometrical distortions due to a varying delay across or along the nonlinear medium, distortions to which single-shot pulse-measurement techniques are essentially immune. And multishot techniques currently cannot measure spatiotemporal distortions.

In singleshot autocorrelation and FROG measurements, on the other hand, the delay is mapped onto the transverse position by crossing replicas of the pulse at a relatively large angle (see Fig. 1). These methods are experimentally considerably simpler than their multishot cousins, they are very easy to align, and they are typically immune to geometrical-smearing effects. Also, they can indicate spatiotemporal distortions: single-shot FROG and GRENOUILLE [2,3] (a simplified version of single-shot FROG) also measure the spatial chirp and pulse-front tilt [4,5]. However, because, in these methods, the spatial coordinate is also used to obtain temporal (delay)

information, it is generally considered necessary to assume nearly constant beam intensity versus the relevant transverse coordinate (say, x). It is well known that this assumption is necessary, and, as a result, even users with moderate-sized fairly smooth Gaussian beam profiles tend to avoid these methods, opting instead for interferometric methods (which, ironically, have considerably more stringent spatial-profile requirements!). In any case, in single-shot FROG and GRENOUILLE measurements, especially of relatively long pulses (which result in relatively broad traces), a complex pulse spatial profile in the delay direction could, in principle, distort the trace and the resulting retrieved pulse temporal profile. Indeed, even an ideal Gaussian beam, if too small, can result in a measured trace and pulse that are too short in time [1]. Thus, it is important to consider the beam's spatial profile at the nonlinear crystal in the delay (x) direction.

GRENOUILLE is also sensitive to the input-beam spatial properties in another manner. In addition to mapping delay onto the x coordinate, GRENOUILLE also utilizes the fact that a second-harmonic-generation (SHG) crystal's phase-matching angle varies with wavelength and that a broadband input beam focused tightly into a thick nonlinear crystal will yield an angularly dispersed second-harmonic output beam [1–3,6]. This is the required spectrometer in GRENOUILLE. Thus the signal-pulse frequency is mapped to the y transverse coordinate. GRENOUILLE thus spectrally resolves the autocorrelation SHG signal by measuring the variations in the nonlinear-optical signal intensity versus angle in the y direction. But variations in the input beam's intensity versus angle at the crystal can also yield such signal variations, which would distort the GRENOUILLE-measured
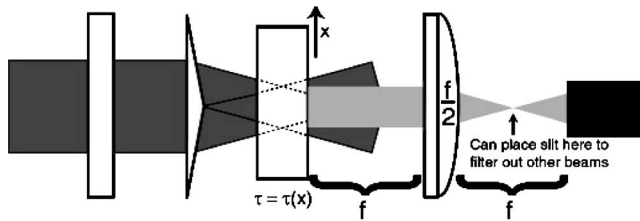
Fig. 1.   Top view of GRENOUILLE.

Fig. 2.   Side view of GRENOUILLE.

trace spectrum. Thus, the input-beam intensity dependence on angle at the SHG crystal in the *y* direction at the nonlinear crystal is also important to take into account.

The purpose of this paper is to model and study the effects of the beam spatial properties on single-shot FROG and, in particular, GRENOUILLE. We compute the effects of the spatial profile on the measured GRENOUILLE trace. We show that, in the absence of spatiotemporal distortions, the effect of the spatial profile on the measured GRENOUILLE trace is simply a spatial intensity mask. The mask can be calculated simply from the measured spatial intensity profile of the input beam (for standard single-shot FROG using a thin crystal, it *is* the spatial profile). Such distortions can be removed by simply dividing the measured FROG or GRENOUILLE trace by this mask.

We find that, due to fortuitous geometrical characteristics of the GRENOUILLE technique, it is considerably less affected by these spatial factors than other methods are. One such characteristic is the fact that, in GRENOUILLE, the beam splitter is a prism, which crosses the left half of the beam with the right half. This yields a spatial mask that is usually the product of an increasing function and a decreasing one, which is then considerably less variable. Also, GRENOUILLE uses a thick crystal, so, as the beams cross in the crystal, they scan across each other transversely, yielding a modified spatial mask that involves a convolution over the simpler form of the mask, smearing out any finely detailed structure. As a result, such effects are generally small (much smaller than generally perceived), and, as a result, we have actually found it difficult to observe any such spatial-intensity-induced distortions in GRENOUILLE measurements.

Finally, because single-shot FROG and GRENOUILLE necessarily incorporate a camera for measuring the pulse spectrogram, they naturally also usually measure the spatial profile of the beam. As a result, it is relatively convenient to take advantage of the spatial information to improve the temporal measurement when necessary.

2. GRENOUILLE

In GRENOUILLE, an input beam propagating in the *z* direction is manipulated differently in the two transverse dimensions, *x* and *y*. In Fig. 1, in the *x* dimension, a Fresnel biprism splits a broad (typically 1 to 2 cm in diameter) beam in two, and the resulting two halves of the beam are crossed by a Fresnel biprism at the SHG crystal. The resulting SH signal is imaged on the detector.

In the *y* dimension, as shown in Fig. 2, a cylindrical lens focuses the beam into the SHG crystal, and the resulting SH signal is passed through a Fourier-

transforming lens that maps the beam output angle to position at the detector (independent of the input position).
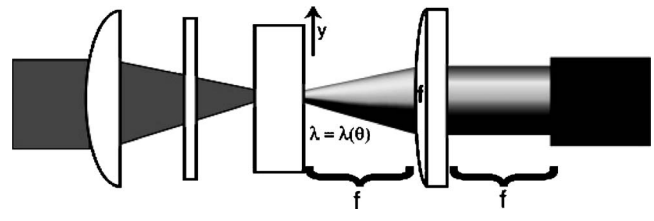
A. Spatial-Profile Effect in the *y* Dimension

We begin with the latter effect. Using simple ray tracing, we can see that, in the wavelength (*y*) direction, the first cylindrical lens converts the spatial profile in that direction, $E_{in}(y)$, into an angular profile, $E_{in}(\theta)$, with $\theta = y/f$, where *f* is the focal length of the lens. Because each incidence angle at the SHG crystal corresponds to a particular phase-matching wavelength, the different frequency components of the SHG signal will be mapped to their respective angles, $E_{out}(\theta)$. The Fourier-transform lens then transforms the angular distribution of the SH signal into a spatial distribution, $E_{out}(y)$, at the camera.

From Fig. 3, it is easy to see that, not only is a given wavelength mapped to a particular position at the camera (by phase matching), but, using simple ray tracing, so is a particular spatial position of the input beam. So, for example, if the input beam has a hole in it at a particular position, no light will be incident at that particular angle on the crystal, and so no output SHG signal will occur in that direction corresponding to that particular wavelength. This is the essence of the spatial-profile effect in this dimension. We neglect the effect of the off-axis SHG and off-axis sum-frequency generation (which were discussed in detail in a previous publication and shown to have little effect [7]).

So we have

$$I_{out}(-\theta) \propto I_{in}^2(\theta).$$

Since $I_{out}(-\theta) \propto I_{out}(y)$, we can relate the input profile, $I_{in}(y)$, to the output profile, $I_{out}(y)$:

$$I_{out}(y) \propto I_{in}^2(-y).$$

Thus, the influence of the input spatial profile of the input beam on the output trace in the *y* dimension is a mul-
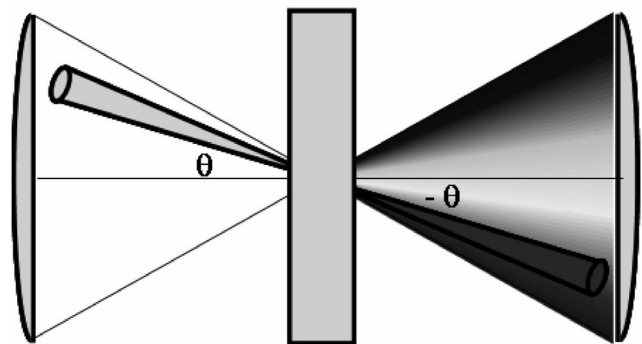
Fig. 3.   Spatial-profile effect in the *y* direction.
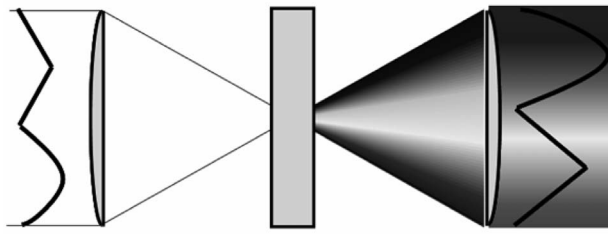
Fig. 4.   Intensity mask introduced by a nonuniform spatial profile in the *y* direction. Note that the spatial mask is the square of the input intensity, and so variations are somewhat amplified.

tiplication of the measured trace by a simple intensity mask, which is the square of the input pulse profile in the *y* dimension, as shown in Fig. 4.

B. Spatial-Profile Effect in the *x* Dimension
In the delay (*x*) direction, GRENOUILLE involves crossing the two halves of the beam at the nonlinear crystal to generate a second harmonic, which is imaged onto a camera. As shown in Fig. 5, only a portion of each half of the beam is typically engaged in signal generation.

As in the *y* direction, the effect caused by the spatial profile of the pulse on the GRENOUILLE trace is simply
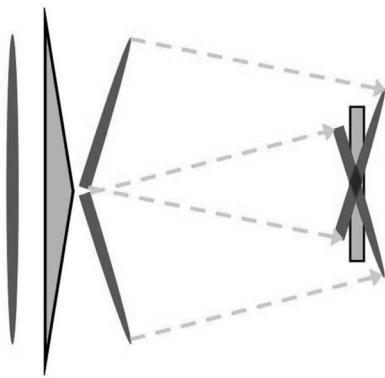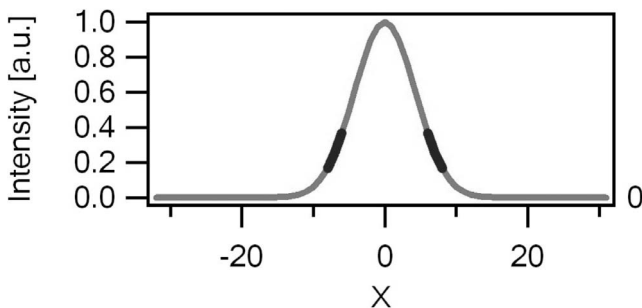
Fig. 5.   Top, two halves of the beam crossed by the biprism, and the overlapping zone on the nonlinear crystal. Bottom, the active spatial portion of the pulse, which takes part in the generation of the second-harmonic signal.
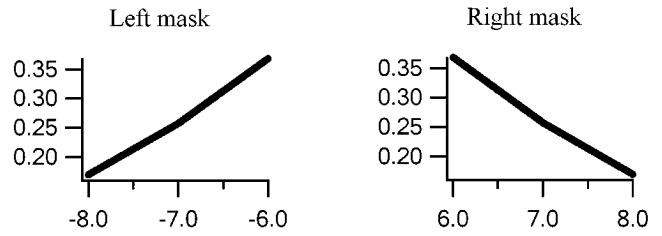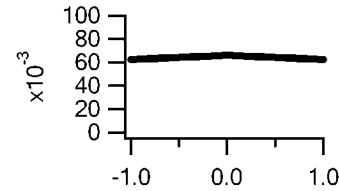
Fig. 6.   Top left, intensity of the active zone on the left half of the beam. Top right, intensity of the active zone on the right half of the beam. Bottom, overall intensity mask due to the spatial profile.

an intensity mask: the product of the intensity of the left half of the beam and that of the right half.

It is not difficult to see that, for a short pulse, if the spatial profile is symmetrical, the thick black regions of each beam in Fig. 6 will be symmetrically placed on the profile. In this case, the overall mask will be nearly constant, and the effect of the spatial profile will be relatively small. On the other hand, it is easy to imagine cases for which the overall mask could not be neglected. First, when the pulse is long, then the relevant regions of the spatial profile will spread over a larger fraction of the spatial profile, and their product will no longer approximate a constant. Second, if the spatial profile is not symmetrical or the relevant zones are located on asymmetrical places of the spatial profile (in the case of a misaligned beam), the contribution from the left and right sides of the beam could vary quite differently.

C. Combined Spatial-Profile Effect in the *x* and *y* Dimensions—Simulations
Combining the *x* and *y* effects, the overall spatial mask for the GRENOUILLE trace is

$$M(x,y) = I(x - L\varphi, -y)I(x + L\varphi, -y),$$

where we have assumed a thin crystal, and $I(x,y)$ is the spatial profile of the input beam, L is the distance from
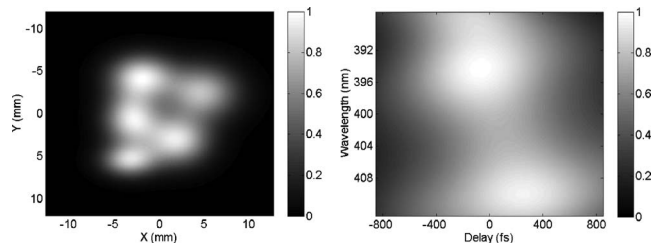
Fig. 7.   Left, example complex input-beam profile. Right, overall intensity mask for it.
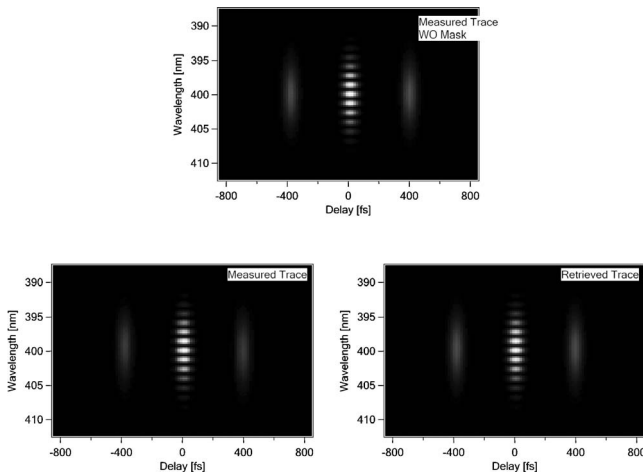
Fig. 8.   Top, exact GRENOUILLE trace for a double pulse. Bottom left, distorted GRENOUILLE trace due to the nonuniform spatial profile of the input beam (shown in Fig. 7). Bottom right, retrieved trace for the double pulse from the spatial-profile-distorted GRENOUILLE trace.

the biprism to the crystal, and 2φ is the crossing angle of the beam.

We now calculate the effect of the 2D spatial mask of a GRENOUILLE trace for various pulses and input spatial profiles. We used the parameters of a commercial GRE-NOUILLE (Swamp Optics, Model 8-50) for the simulations, which has a cylindrical lens with a focal length of 150 mm and a Fresnel biprism with a 170° apex angle.

First, consider the complex input-beam profile shown in Fig. 7. The corresponding intensity mask is also shown in Fig. 7. We consider a double pulse, whose trace is given in Fig. 8, which also shows how this trace will be modified by the above mask due to the structured spatial profile. Figure 9 shows the exact and retrieved pulses in the time and frequency domains. Note that, even though the FROG error for the pulse retrieval from the spatial-profile-distorted 128×128 trace was large (1.4%), the retrieved intensity and phase actually converged to a waveform closely resembling the correct pulse.

For another example, consider an inappropriately small input beam with a Gaussian profile, approximately 0.33 mm, and after the (×6) telescope in the GRE-NOUILLE, the beam diameter will still be only 2 mm, much smaller than is considered appropriate for an accurate measurement. The corresponding intensity mask is shown in Fig. 10. With this mask, we tested two pulses.
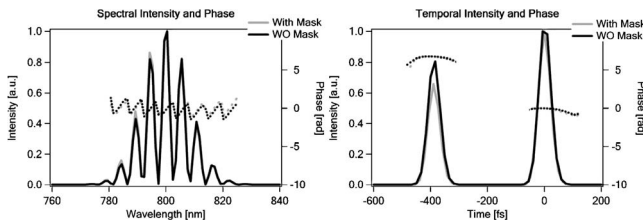
Fig. 9.   Correct intensity and phase for the double pulse and also the retrieved intensity and phase for the double pulse with the spatial-profile-induced trace distortions. On the left are the spectral intensity and phase; on the right are the temporal intensity and phase. Note that the distortions in the retrieved double pulse due to the nonuniform spatial profile are not severe, despite the very poor spatial profile used.
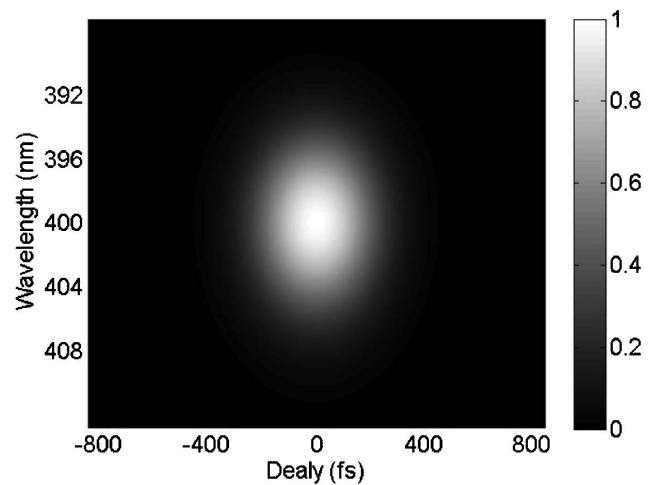
Fig. 10.   Overall intensity mask for a 2 mm Gaussian beam in the GRENOUILLE example.
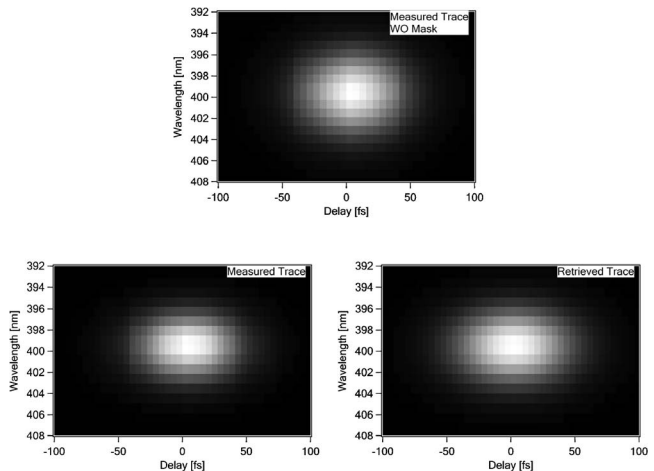
Fig. 11.   Top, exact GRENOUILLE trace for a transform-limited pulse. Bottom left, distorted GRENOUILLE trace due to the non-uniform spatial profile of the input beam (shown in Fig. 10). Bottom right, retrieved trace for the transform-limited pulse from the spatial-profile-distorted GRENOUILLE trace.
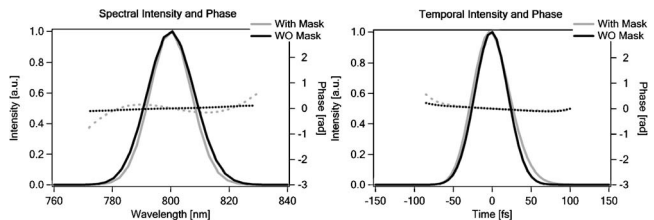
Fig. 12.   Retrieved intensity and phase of the transform-limited pulse with the spatial mask and without the spatial mask for comparison. On the left are the spectral intensity and phase; on the right are the temporal intensity and phase.

The first was a transform-limited Gaussian pulse and the other was a chirped pulse. Under this spatial-profile mask, a GRENOUILLE trace of the transform-limited pulse is modified as shown in Fig. 11. The retrieved pulse and its trace are shown in Figs. 11 and 12. The FROG error for the pulse retrieval from the distorted 128×128 trace was approximately 0.93%, which is actually indicative of a fairly good measurement. Because the mask has reduced the already small-area trace to below that al-
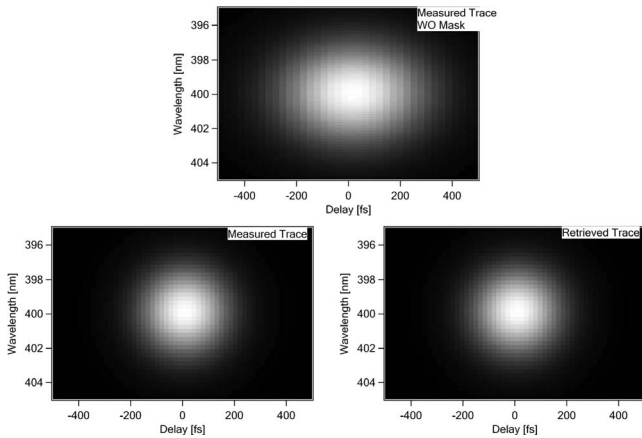
Fig. 13. Top, exact GRENOUILLE trace for a chirped pulse. Bottom left, distorted GRENOUILLE trace due to the nonuniform spatial profile of the input beam (shown in Fig. 10). Bottom right, retrieved trace for the chirped pulse from the spatial-profile-distorted GRENOUILLE trace.

lowed by the uncertainty principle, the FROG algorithm recognizes the distorted trace as too small, and it retrieves a pulse that has a larger trace area. Of course, the algorithm cannot know whether to increase the spectral width or pulse length, so the choice yields some error, but considerably less than what might be expected. In general, however, one should be careful in this case since the algorithm cannot know which direction in which to expand the trace. Correction of the trace using the spatial mask is advised in this case (see Section 3). When the pulse is chirped, the modification by the spatial mask is more significant, as shown in Fig. 13. The retrieved trace and pulse are shown in Figs. 13 and 14. The FROG error for the distorted 128×128 trace was small (0.09%), even though the retrieved intensity and phase did not accurately match that of the pulse we generated. This is because the trace modified by the spatial mask does not violate the uncertainty principle as in the previous example and so appears legitimate and the corresponding pulse was retrieved inaccurately by the algorithm, as shown in Fig. 14.

For another example, suppose that we have a very fine-structured beam profile, as shown in Fig. 15, which also shows the corresponding mask. Under this mask, a GRENOUILLE trace for the above chirped pulse will be modified as shown in Fig. 16. Even though the FROG error for the 128×128 traces was large (1.79%), the retrieved intensity and phase of the pulse almost perfectly matches that of the actual pulse, shown in Fig. 17. This is because
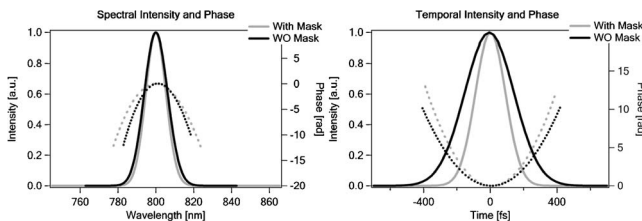
Fig. 14. Retrieved intensity and phase of the chirped pulse with the spatial mask and without the spatial mask for comparison. On the left are the spectral intensity and phase; on the right are the temporal intensity and phase. Note the shorter pulse and narrower spectrum due to the small beam.
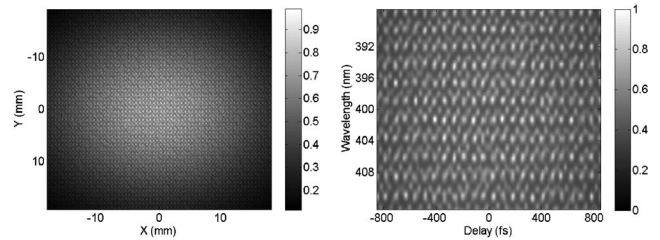
Fig. 15. Left, fine-structured input-beam profile. Right, intensity mask for the fine-structured beam spatial profile.
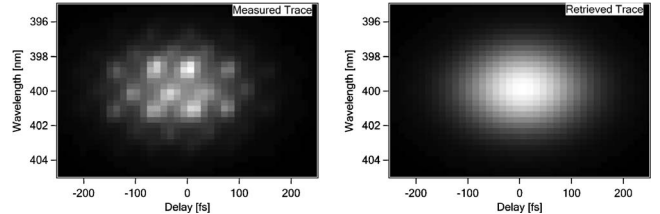
Fig. 16. Left, distorted GRENOUILLE trace for the chirped pulse (of Figs. 13 and 14) due to the nonuniform spatial profile of the input beam shown in Fig. 15. Right, retrieved trace for the chirped pulse from the spatial-profile-distorted GRENOUILLE trace.
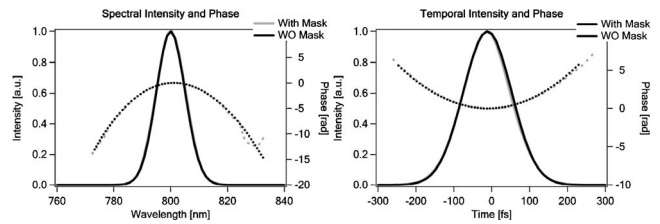
Fig. 17. Exact intensity and phase and retrieved intensity and phase of the chirped pulse from the trace distorted by the fine-structured input beam (shown in Fig. 15). On the left are the spectral intensity and phase; on the right are the temporal intensity and phase. Note that the algorithm sees through the unrealistic (uncertainty-principle-violating) structure in the trace and finds almost precisely the correct pulse.

the fine structure induced by the mask in the trace is too fine and again violates the uncertainty principle. The algorithm therefore could not reproduce it and so ignored it, yielding a very good measurement, despite seemingly debilitating spatial structure in the beam.

D. Extension to a Thick Nonlinear Crystal
The above analysis assumed a thin SHG crystal, which will be valid in SHG FROG devices built using Fresnel biprisms, bimirrors, or other optics that split the beam in half spatially. Such devices are common, and they are used for all pulse-length ranges, and especially for sub-20-fs pulses and pulses longer than a few picoseconds, for which the thick-crystal spectrometer is either too dispersive in time or not dispersive enough in angle. For commonly used GRENOUILLE devices, which incorporate a several-millimeter-thick crystal for spectral resolution, there is another effect that further reduces the effect of the spatial mask. As the pulses cross and propagate through the thick medium, they slide across each other (see Fig. 18). To understand this, consider a very thick crystal. When the pulses first meet (usually before the crystal entrance face but possibly even at it), the left edge
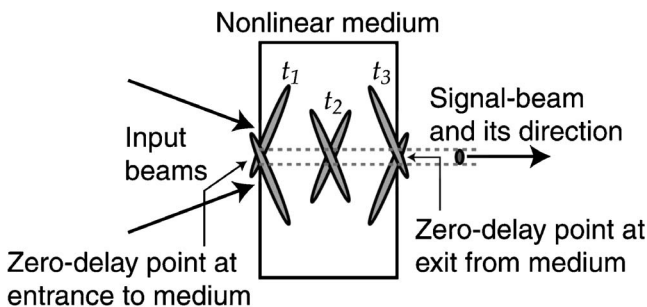
Fig. 18.   Beam geometry showing the two crossed beams at three distinct times as they propagate through the nonlinear medium. Note that the signal beam propagates along the bisector of the input beam angle. Also, along the dashed line (and all other lines parallel to it), the same relative beam delay occurs for the entire length of the medium. Thus, no geometrical smearing-type distortion is present; the signal pulse shown reveals the resulting (accurate) width of the trace. For our purposes, however, note that, spatially, the two pulses slide across each other as they propagate through the medium. This has the effect of smearing out any distortions due to any spatial structure in the input beam. (Figure and part of the caption reprinted with permission from [1].)

of one pulse just touches the right edge of the other. As they propagate through the crystal and exit from it, the overlap regions will slide along each beam until finally the pulses cease to overlap in space, at which point the right edge of the one pulse will overlap the left edge of the other. The effect of this is to smear out the distortions due to spatial structure in the input beams, further improving the resulting trace, despite possible beam spatial structure.

To model this effect, we simply integrate across the beam profiles for the range of positions that will see such overlap due to the thicker crystal. The mask then becomes

$$M(x,y) = \int_{-L/2}^{L/2} I(x - L\varphi - z \sin \varphi, -y)$$
$$\times I(x + L\varphi + z \sin \varphi, -y)\mathrm{d}z.$$

We see that this effect is a convolution of the spatial profile with itself over the region of the beam for which such sliding occurs. The fraction of the beam over which this convolution occurs, that is, the fraction of the beam that is averaged in the above integral, is $L \sin(\varphi)/d$, where d is the beam diameter at the SHG crystal (~ 1 cm), φ is $\sim 10°$, and L is the crystal thickness (3.5 mm). For the commercial GRENOUILLE that we used for these studies, the fraction of the beam over which this convolution occurs is
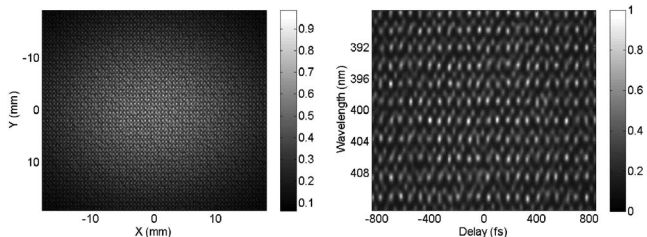
Fig. 19.   Left, fine-structured input-beam profile used in our simulation. Right, overall intensity mask for a thin crystal (not including the convolution effect).
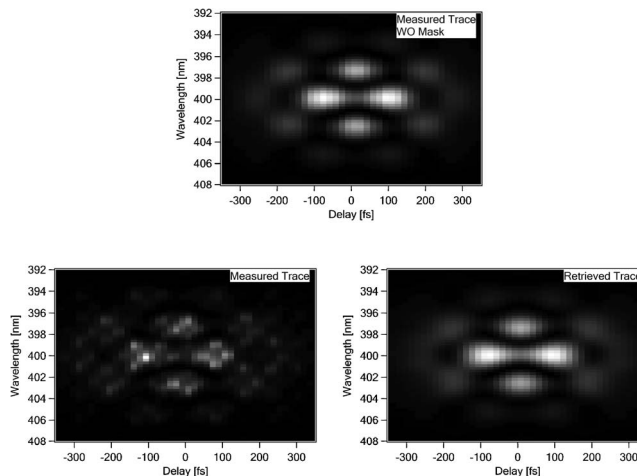
Fig. 20.   Top, exact GRENOUILLE trace for a double-chirped pulse. Bottom left, distorted GRENOUILLE trace due to the non-uniform spatial profile of the input beam (shown in Fig. 15). Bottom right, retrieved trace for the double-chirped pulse from the spatial-profile-distorted GRENOUILLE trace.

$\sim 10\%$, which is significant. So this longitudinal smearing of the spatial profile could easily smear out large spikes in the beam in many cases, especially if there are many of them.

Thus if the crystal is thick enough, even a very complex spatial profile could yield accurate results due to the combination of the algorithm's ability to unrealistically structure in the trace and the convolution effect to suppress it in the first place. For example, consider the fine-structured beam profile shown in Fig. 19, which also shows the corresponding intensity mask—not including the convolution effect. Under this mask, a GRENOUILLE trace for a relatively complex pulse will be modified as shown in Fig. 20. Even though the FROG error for the distorted 128×128 trace was large (2.12%), the retrieved intensity and phase converged to a very reasonable pulse, as shown in Fig. 21. However, looking at the trace, it is clear that noise could easily affect the retrieval, and improved trace quality would be desired in practice.

If, however, we include the convolution effect due to the thick crystal in GRENOUILLE, the corresponding intensity mask is shown in Fig. 22. Note that the intensity fluctuations in this mask are less than those of the mask in Fig. 19.
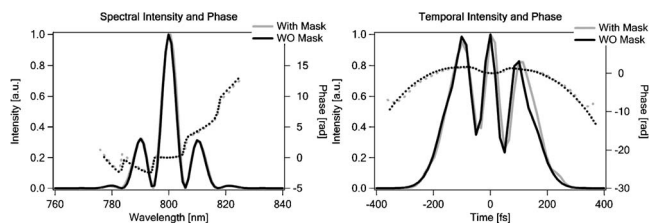
Fig. 21.   Retrieved intensity and phase of a double-chirped pulse with the spatial mask and without the spatial mask for comparison. On the left are the spectral intensity and phase; on the right are the temporal intensity and phase. Note that, despite the severe complex structure in the beam and its corresponding spatial mask, very good results were obtained, mainly due to the algorithm seeing through the unrealistic structure of the trace induced by the mask.
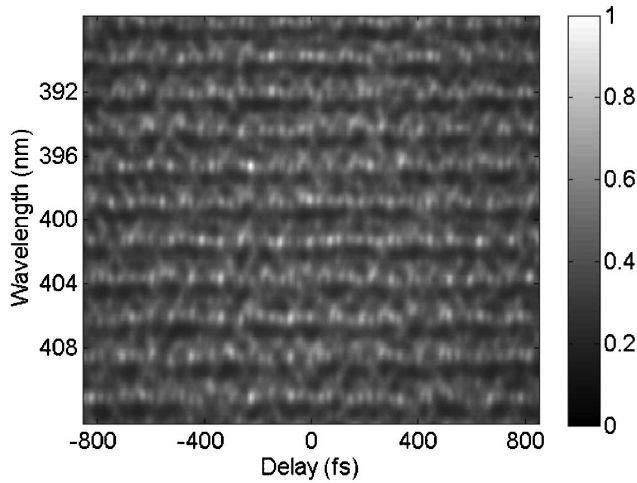
Fig. 22. Overall intensity mask for a thick crystal.

Under this mask, a GRENOUILLE trace will be modified as shown in Fig. 23. Even though the FROG error for the 128×128 traces is still large (1.85%), it is less than that for the previous case without the thick crystal and its corresponding convolution, and the retrieved intensity and phase converged to reasonable results, shown in Fig. 24. This trace will in practice be much less susceptible to the deleterious effects of noise.

3. EXPERIMENT

We tested the above analysis using a commercial GRE-NOUILLE (Swamp Optics, Model 8-50). A KM Labs Ti:sapphire oscillator provided a stable train of ~ 130 fs pulses. We then measured the pulse train twice, once with a beam-magnifying ($\times 2$) telescope in the beam and again with the telescope reversed to yield a beam-reducing telescope ($\times 0.5$). Because the GRENOUILLE incorporates an internal $\times 6$ telescope, the beam-expanded large beam easily spanned the required delay and spectral ranges of the device with an effectively uniform intensity. But the beam-reduced small beam was too small to span the required delay range and the required spectral range. The small-beam case was in some sense a worst-case scenario because reducing the beam any further yielded diffraction-induced beam expansion inside the device (before the telescope), effectively increasing the beam diameter at the crystal.

We found it difficult to see these effects using unchirped ~ 130 fs long, 7.7 nm bandwidth pulses directly
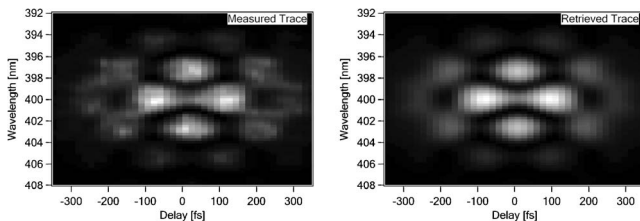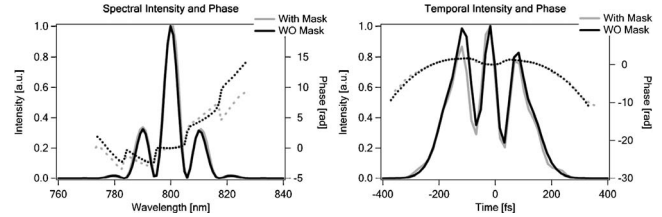
Fig. 24. Retrieved intensity and phase of the double-chirped pulse with the spatial mask and without the spatial mask for comparison. On the left are the spectral intensity and phase; on the right are the temporal intensity and phase.

from our laser, so we stretched (chirped) the pulse to 205 fs in length. The crystal was 4 mm wide, and the beam crossing angle was 4.5°. The desired delay range across the crystal was at least 600 fs. We measured the spatial profile of the beam using the spatial profile camera of the GRENOUILLE, yielding the spatial mask (for the smaller beam) shown in Fig. 25. Although the crystal was 3.5 mm thick, the beam was fairly smooth, and the thick-crystal convolution yielded a negligible effect on the mask. Using the larger of the two beams, the beam size at the crystal was 18 mm. The beam size using the smaller beam was one fourth this amount, or 4.5 mm. Because the delay across the crystal was 264 fs/mm, the small beam introduces some distortion into the trace, as shown in Fig. 26. In the y direction, the phase-matching wavelength varied with angle at the rate of 27 nm/deg. The large beam size yielded a full divergence angle of 3.4°, so it also yielded an available spectral range of 93 nm, considerably greater than the bandwidth of our pulse. However, the smaller beam yielded an available spectral range of only one fourth as much, and so it provided slight cropping of the trace in the spectral direction (see Fig. 26). The corrected results are shown in Fig. 27. After the correction, the measured bandwidth increased to 7.4 nm, and the pulse duration increased to 207 fs for the small beam, which compares well with the bandwidth, 7.7 nm, and pulse length, 205 fs, measured using the large beam.

4. DISCUSSION AND CONCLUSIONS

We find that, especially in GRENOUILLE, there are several ameliorating aspects to the spatial-profile effect that minimize its detrimental effects in single-shot pulse measurement. First, a usually increasing function of space from one beam crosses a generally decreasing function of space from the other. This generally results in a nearly constant contribution to the spatial mask for typical

Fig. 23. Left, distorted GRENOUILLE trace for the double-chirped pulse due to the nonuniform spatial profile of the input beam (shown in Fig. 15) now including the thick-medium convolution effect. Right, retrieved trace for the chirped pulse from the spatial-profile-distorted-and-convolved GRENOUILLE trace.
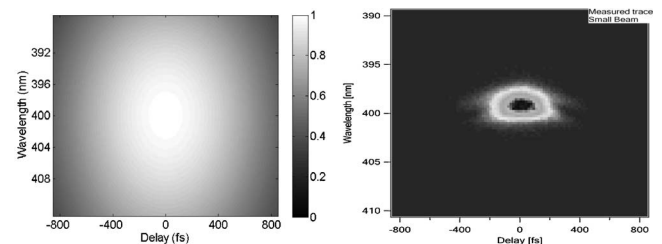
Fig. 25. Left, measured spatial mask. Right, the FROG trace for our measurements when using the smaller beam. Note that the spectral range is sufficient to correctly measure the trace, but the temporal range is not.
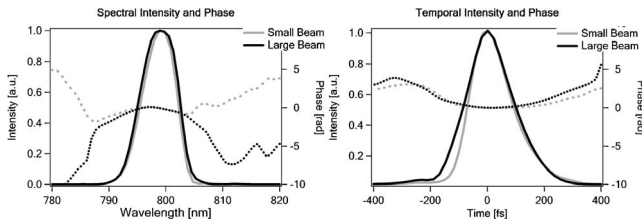
Fig. 26.   Left, measured spectrum and spectral phase using the large and small beams. Right, measured intensity and phase versus time using the large and small beams. Note the slightly shorter pulse and narrower spectrum due to the small beam.

smooth beam profiles. Second, the autoconvolution that occurs due to the thick crystal in GRENOUILLE further smears out the mask, especially if the beam has fine structure or hot spots. In addition, another effect that also acts to hide the spatial-profile effect is the massive over-determination of the pulse intensity and phase by the measured FROG trace. Any systematic error due to the spatial-profile (or other) effect in a trace with significant structure due to an interesting pulse shape, such as that due to a double pulse, cannot correspond to a real pulse and so is generally ignored by the FROG algorithm. The result is that such systematic error does not affect the pulse as much as one might think.

Thus, especially if the crystal is thick, even a very complex spatial profile will likely still yield accurate results. Indeed, we found it difficult to observe the effect at all in the laboratory, and our experience with numerous such devices previously is that the effect is indeed rare. Even extremely complex beams from amplifier systems usually yield accurate measurements due to the convolution and resulting smearing out of hot spots in the beam.
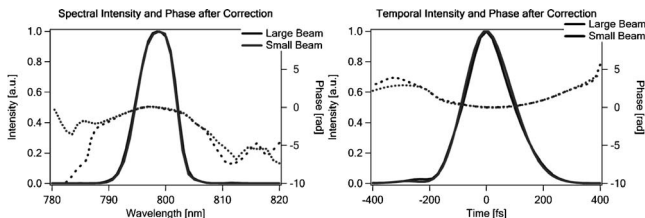
Fig. 27.   Large-beam results and corrected small-beam results using the spatial mask. Note the improved agreement between the two measurements.

Of course, pulses with extremely complex spatial profiles are likely to have different intensities and phases versus time across their complex spatial profile and so should not be measured using any technique that assumes a single intensity and phase, independent of position, despite the several ameliorating circumstances that we have seen occur in GRENOUILLE.

The only case in which the spatial profile effect is likely to cause problems is that of a pulse with a FROG trace that is very broad in both time and frequency (e.g., a highly linearly chirped smooth-intensity pulse) with a beam that has broad and large variations over its spatial profile, such as a pure TEM_{nm}, where n and m are small numbers, as in our first simulated example. And even in that case, it should be possible to correct for the variation by simple division by the mask. Of course, zeroes in the spatial intensity cannot be corrected, but the convolution due to GRENOUILLE's thick crystal can fill in the zeroes and even overcome this problem.

Keeping these effects in mind should allow the use of these methods in a wider range of applications and will further improve their accuracy.

REFERENCES

1. R. Trebino, *Frequency-Resolved Optical Gating: The Measurement of Ultrashort Laser Pulses* (Kluwer Academic, 2002), Chap. 6, 7.
2. P. O'Shea, S. Akturk, M. Kimmel, and R. Trebino, "Practical issues in the measurement of ultrashort pulses using GRENOUILLE," Appl. Phys. B **79**, 683–691 (2004).
3. P. O'Shea, M. Kimmel, X. Gu, and R. Trebino, "Highly simplified device for ultrashort-pulse measurement," Opt. Lett. **26**, 932–934 (2001).
4. S. Akturk, M. Kimmel, P. O'Shea, and R. Trebino, "Measuring pulse front tilt in ultrashort pulses using GRENOUILLE," Opt. Express **11**, 491–501 (2003).
5. S. Akturk, M. Kimmel, P. O'Shea, and R. Trebino, "Measuring spatial chirp in ultrashort pulses using single-shot frequency-resolved optical gating," Opt. Express **11**, 68–78 (2003).
6. C. Radzewicz, P. Wasylczyk, and J. S. Krasinski, "A poor man's FROG," Opt. Commun. **186**, 329–333 (2000).
7. X. Liu, R. Trebino, and A. V. Smith, "Numerical simulations of ultrasimple ultrashort-laser-pulse measurement," Opt. Express **15**, 4585–4596 (2007).